Ultrafast electron scattering from surface to bulk states at the InP(100) surface

Philipp Sippel,[1,*] Jodi M. Szarko,[2] Thomas Hannappel,[3] and Rainer Eichberger[1]

[1]*Helmholtz-Zentrum Berlin für Materialien und Energie, Institute for Solar Fuels, Hahn-Meitner-Platz 1, D-14109 Berlin, Germany*

[2]*Lafayette College, Department of Chemistry, Easton, Pennsylvania 18042, USA*

[3]*Technische Universität Ilmenau, Institut für Physik, Postfach 100565, D-98684 Ilmenau, Germany*

(Received 13 November 2014; revised manuscript received 21 January 2015; published 23 March 2015)

We investigated the scattering dynamics of hot electrons at the atomically well-defined In-rich (2×4)-reconstructed InP(100) surface in the presence of different surface states. Using energy- and time-resolved femtosecond two-photon photoemission spectroscopy, we determined the electron transfer between three-dimensional bulk states and the two-dimensional surface state C2, located high above the conduction band minimum (CBM) avoiding energetic overlap with relaxed bulk electrons. At excitation energies, where C2 was populated through hot bulk electrons, relaxing towards the CBM, we found evidence that the energy loss rate of the photoexcited electron distribution is mostly determined by inelastic electron-phonon scattering between bulk states. This was confirmed by measurements repeated after quenching the surface states with oxygen. For resonant photoexcitation, on the other hand, we measured a time constant of $\tau_{\text{fast}} = 20$ fs for the depopulation of C2, showing that electron-phonon scattering between bulk and surface states might have direct consequence on ultrafast relaxation dynamics for materials with a high surface-to-bulk ratio.

DOI: 10.1103/PhysRevB.91.115312 PACS number(s): 63.20.kd, 73.20.At, 78.47.J−, 79.60.Bm

I. INTRODUCTION

InP is a model system for studying electron-phonon interactions and the cooling dynamics of hot electron distributions in compound semiconductors, as well as an essential material component of high-performance optoelectronic devices [1,2]. Time-resolved optical methods such as photoluminescence or transient absorption spectroscopy have been applied extensively to investigate the fundamental physical aspects of bulk electron dynamics [3–6]. Due to the trend towards smaller and low-dimensional devices, however, the surface and interface properties become increasingly important and substantially influence the electron dynamics in these materials [7–9]. Moreover, chemical reactions in the presence of semiconductor surfaces, such as photocatalytic water splitting, depend critically on the electronic properties and charge carrier dynamics at the surface [10]. The above-mentioned optical methods, however, are sensitive mostly to the bulk properties and consequently there are still little data available regarding the actual charge carrier dynamics at semiconductor surfaces and the influence of surface states on the electron cooling process. An appropriate method to study electron dynamics at surfaces is time-resolved femtosecond two-photon photoemission spectroscopy [11,12] (tr-2PPE). Here, a laser pulse (pump) excites electrons to an intermediate state and a second pulse (probe) promotes them above the vacuum level with a kinetic energy signature related to their interim binding energy. This allows measuring the temporal evolution of the photoexcited electron distribution directly and has already been applied to investigate the electron dynamics at various semiconductor surfaces. However, most studies focused on the underlying bulk electron dynamics [13–17], while surface state related studies are almost exclusively to be found for silicon [12,18].

An exception are the experiments by Töben *et al.* on the electronic properties and electron dynamics of well-defined InP(100) surfaces [19–21], i.e., the P-rich and the In-rich (2×4) surface reconstructions, that were investigated in very much detail [22–26], the latter having also been used as a functionalized part of applications such as in water splitting devices [2,27]. Its unit cell can be recognized by a buckled In-P dimer on top of an In layer and resembles the atomic surface structure of the Ga-rich (2×4)-reconstructed surface of GaP(100) that has also been in the focus of several recent experimental and theoretical studies of surface chemistry [10,28–30].

Three different surface states have been detected on In-rich InP(100) [19,22]: an occupied state V1, 0.1 eV below the valence band maximum (VBM), and two unoccupied states C1 and C2, which are 0.25 and 0.85 eV above the conduction band minimum (CBM), respectively. So far, the electron dynamics of only C1 have been investigated with tr-2PPE and theoretical *ab initio* calculations [20,21]. However, the depopulation dynamics, i.e., the scattering of electrons from the low-energetic surface state C1 to energetically adjacent bulk states could not be resolved because of the superimposed high-energy tail of the photoexcited bulk electron distribution. The measurements thus reflected only the cooling of the hot carrier distribution with a rate constant of $(1/7)$ ps^{-1} instead of the depopulation of C1 [20].

In this work, in contrast, we focus on the high-energetic surface state C2 using tr-2PPE, which is associated with dangling bonds of the second layer of In atoms [22,31] at the same InP(100) surface reconstruction. This greatly reduces the influence of the photoexcited bulk electron distribution that is centered at lower energies, thus allowing us to discriminate the depopulation dynamics of C2 from the cooling of the bulk electron distribution.

We chose two different excitation schemes with respect to the applied laser pump energy. Accordingly, C2 was either populated indirectly by relaxing bulk electrons that were photoexcited high into the conduction band, or directly

*philipp.sippel@helmholtz-berlin.de

by resonant optical excitation. Hence, scattering processes from surface to bulk states as well as the scattering from bulk to surface states could be investigated, separately. Both experiments were conducted before and after exposing the sample to oxygen and thus quenching C2 completely. This enables us to extract the dynamics corresponding to the surface from the remaining bulk-related background signal and also shows how quenching of the surface states directly affects the electron dynamics.

II. EXPERIMENT

InP films were grown with tertiarybutylphosphine and trimethylindium as precursors by metal organic vapor phase epitaxy (MOVPE) employing H_2 as the carrier gas. Nominally undoped layers (background doping of about $n = 1 \times 10^{15}$ cm^{-3}) were grown on n-type InP(100) substrates ($n = 2 \times 10^{18}$ cm^{-3}). Well-established growth parameters ensure a reproducible preparation of the well-ordered (2×4)-reconstructed InP(100) surface [23]. A commercial MOVPE reactor from Aixtron was modified at the sample exit to achieve an extremely fast transfer of the sample to a connected intermediate UHV chamber. We used a patented specific contamination-free UHV shuttle system [32] to commute between the preparation and the tr-2PPE measurement chamber in the nearby laser laboratory.

Ultrashort visible (VIS) and ultraviolet (UV) pulses were generated from two home-built low-power noncollinear optical parametric amplifiers [11] (NOPAs) pumped by a Coherent RegA 9050 regenerative amplifier operating at a repetition rate of 150 kHz. The first NOPA was tuned to $h\nu = 2.33$ eV to generate the VIS light. The output of the second NOPA was set to either 515 or 540 nm and subsequently frequency doubled in a 75-μm-thick β-barium borate crystal to deliver UV pump/probe pulses with $h\nu = 4.82$ or 4.55 eV, respectively, depending on the type of experiment. For the time-resolved measurements, the UV beam was split, with one part being used as the probe beam and passed through a high-resolution optical delay line. The optical path for the pump beam, either the other part of the UV beam or the VIS beam, was kept constant. When pumping with VIS light, the photon flux for the VIS beam was typically 2.9×10^{13} cm^{-2} per pulse while the UV probe beam was kept at roughly 4×10^{10} cm^{-2} per pulse. In the one-color pump/probe scheme we used a photon flux of about 5.5×10^{11} cm^{-2} per pulse for both UV beams. The chirp, generated in the NOPAs, was compensated for using standard prism lines, achieving an overall time resolution better than 45 fs. This was checked with two-pulse correlation tr-2PPE experiments, exploiting two-photon absorption on a freshly sputtered Cu(111) crystal [33].

The incoming light beams hit the sample at an angle roughly 45° to the surface normal. Only electrons photoemitted normal to the surface were collected using a cone angle time-of-flight (TOF) spectrometer with a length of 313 mm. This means basically that only electrons along the [100] axis in the Brillouin zone can be detected for (100) surfaces, as all other electrons have nonzero transversal momentum. An accelerating bias voltage <0.7 V was applied in the tr-2PPE experiments to detect electrons with low kinetic energy that would otherwise not reach the detector. A work function of ≈4 eV was measured for In-rich InP(100), by applying a bias voltage of 1 V, and checked with ultraviolet photoemission spectroscopy, using a helium lamp. The time delay and the TOF signals were monitored simultaneously, generating both temporally and energetically resolved signals with an overall energetic resolution of approximately 150 meV.

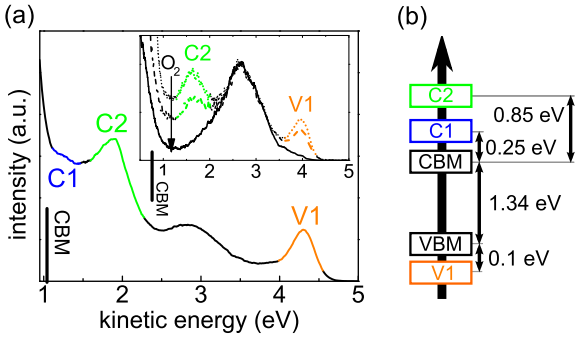

FIG. 1. (Color online) Assignment of surface states to peaks in 2PPE spectra. (a) 2PPE spectrum, using only one laser beam with $h\nu = 4.82$ eV. Peaks associated with the surface states C1, C2, and V1 have been highlighted. Inset: 2PPE spectrum for $h\nu = 4.55$ eV, after different stages of O_2 exposure. From top to bottom: no O_2, 0.3×10^3 mbar s, 1.5×10^3 mbar s. (b) Energetic position of the surface states, identified with 2PPE in Ref. [19].

III. RESULTS

Figure 1(a) shows the kinetic energy spectrum of the In-rich (2×4) InP(100) surface reconstruction that was measured by illuminating the sample with only one pulsed UV beam ($h\nu = 4.82$ eV). This gives rise to 2PPE signals that result from electrons that have absorbed two photons within the duration of an individual laser pulse. The energetic positions and the spectral widths of the pronounced peaks relate to the superposition of all involved transitions at this laser pump wavelength and contain information of initial, intermediate, and final states. Most interesting for this study are the peaks labeled V1, C1, and C2 that have been related to surface states of this specific surface reconstruction in previous experiments [19] and calculations [22,31].

We illustrated the energetic positions of these surface states with respect to the bulk band edges in Fig. 1(b). V1 was attributed to two-photon absorption from an occupied state 0.1 eV below the VBM, leading to the photoemission of electrons in the high kinetic energy range. The peaks of C1 and C2 correspond to unoccupied surface states 0.25 and 0.85 eV above the CBM, respectively. These states are populated by electrons, photoexcited with the pump laser pulse. In a second subsequent photon absorption process within the duration of the same laser pulse, the corresponding excited electrons are photoemitted, leading to the appearance of the mentioned peaks in the kinetic energy spectrum. In particular we used the prominent peak C2 as a reference to allocate the CBM in our spectra, according to Töben *et al.* [19], exactly 0.85 eV below C2. The broad peak with a maximum at $E_{kin} \approx 2.8$ eV originates from intermediate bulk states, populated via interband transitions [19].

The photon energy of $h\nu = 4.82$ eV was applied to get an overview of the different surface states. However, we found that a lower photon energy of $h\nu = 4.55$ eV is better suited for time-resolved measurements which aim at the surface dynamics specifically of C2. Most importantly, this reduces the influence of the broad background, caused by single-photon photoemission events (1PPE), which would otherwise overlap energetically with the signal originating from C2. A corresponding kinetic energy spectrum with $h\nu = 4.55$ eV is shown in the inset of Fig. 1(a). Here, the C2 peak remains clearly visible at $E_{kin} \approx 1.6$ eV but C1 has disappeared. Exposing the sample to oxygen, a procedure that is known to quench the surface states at the InP(100) surface [34], leads to the complete disappearance of all surface state related features. This can be seen in the inset of Fig. 1(a), where also measurements are shown that were recorded after different stages of O_2 exposure and normalized to the amplitude of the bulk peak that is not affected.

To study the filling of C2 by electrons that relax from high energetic bulk states, we performed time-resolved 2PPE experiments with two beams (pump and probe) and a variable time delay between both pulse trains. In this first particular measurement, the pump beam has the same photon energy as the probe beam ($h\nu = 4.55$ eV) to fill states high above the CBM. The contour plot in Fig. 2(a) displays the electron count rate versus kinetic energy and time delay for the clean surface, after removal of a static background of photoelectrons that are emitted by the individual beams. For a time delay of $\Delta t = 0$, i.e. when both pulses overlap on the sample at the same time, the kinetic energy spectrum resembles the spectrum that is obtained when only a single laser beam is used [cf. inset of Fig. 1(a)]. The most pronounced signals are the prominent

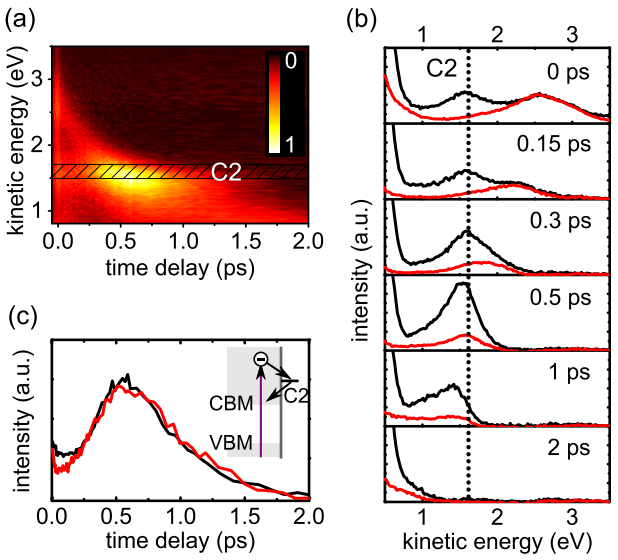

FIG. 2. (Color online) tr-2PPE measurement with $h\nu_{pump} = h\nu_{probe} = 4.55$ eV. (a) Contour plot of the unexposed surface, with the kinetic energy corresponding to C2 indicated with a striped bar. The color represents the normalized count rate. (b) Spectra for different pump probe delays for the unexposed (black) and the O_2-exposed surface (red). (c) Normalized transients before (black) and after (red) oxygen exposure for the energy level of C2, indicated in (b) with a dotted line.

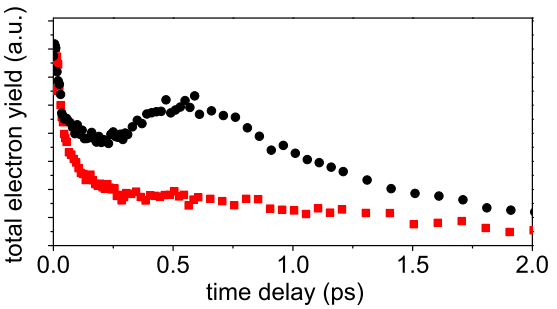

FIG. 3. (Color online) Total electron yield of the tr-2PPE spectra recorded with $h\nu_{pump} = h\nu_{probe} = 4.55$ eV as a function of time delay before (black) and after (red) O_2 exposure.

bulk peak centered at $E_{kin} = 2.57$ eV and the C2 peak at $E_{kin} \approx 1.60$ eV.

The contour plot shows how the pump-induced electron distribution relaxes to lower energies and towards the CBM at $E_{kin} \approx 0.75$ eV by transferring excess energy to the atomic lattice. The bulk peak maximum shifts to lower energies most rapidly and after ≈200 fs we see a drastic increase of the photoelectron yield centered at C2 that attains its maximal value at $\Delta t \approx 580$ fs. We interpret this as electrons that scatter from bulk states to C2 due to phonon emission or absorption.

To verify this, the experiment was repeated after quenching the surface states with oxygen. In Fig. 2(b), we compare spectra for different time delays between the pump and probe pulses, recorded before (black) and after (red) oxygen exposure. The cooling of the bulk electron distribution looks similar within the first 200 fs. However, the measurement recorded after O_2 exposure lacks the prominent 2PPE signal enhancement at the C2 energy level. Instead, the electron distribution continues to relax towards the CBM at $E_{kin} \approx 0.75$ eV with a total electron yield that is rather constant, compared to the drastic increase, which is observed for the sample before O_2 exposure. This can be seen in Fig. 3, where the integral measured number of electrons is plotted against the pump probe delay. A rise of the signal is clearly present before oxygen exposure but absent afterwards, which reinforces our argument of an enhanced photoemission from C2. Hereby, only electrons with $E_{kin} > 0.7$ eV were taken into account to avoid the influence of 1PPE and secondary electrons. While the strong signal enhancement is well represented in the total electron yield, this quantity must be treated with care since it is also subject to effects such as electron diffusion into the bulk as well as electron scattering into side valley states, which are invisible to 2PPE, when only measuring electrons photoemitted normal to the surface.

In order to analyze the population and depopulation dynamics of C2, we compare transients of the corresponding kinetic energy range before and after O_2 exposure in Fig. 2(c). The curves were normalized to their maximum value. For early times the signal from the clean surface is slightly larger due to an initial population of C2. However, for longer time delays both curves are almost identical and resemble the total electron yield curve for the sample before O_2 exposure. This indicates that the cooling rate of the electron distribution does not notably change on this time scale by the presence of C2 but is instead determined by the relaxation of the bulk electron distribution. The scattering in and out of the surface

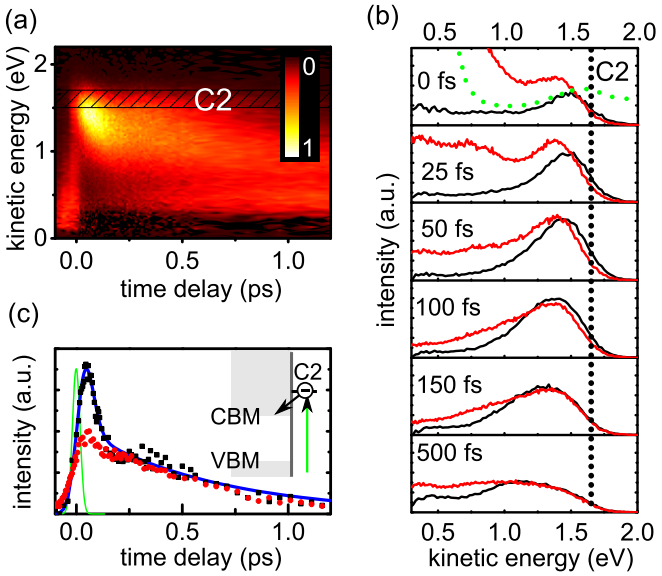

FIG. 4. (Color online) tr-2PPE measurement with $h\nu_{pump} = 2.33$ eV and $h\nu_{probe} = 4.55$ eV. (a) Contour plot before O_2 exposure. C2 indication and color as in Fig. 2(a). (b) Spectra for different Δt before (black) and after O_2 exposure (red). The green dotted line is the spectrum, generated by illuminating with the probe only [cf. inset Fig. 1(a)]. (c) Transient signal for the energy level of C2, indicated in (b) with a black dotted line, before (black squares) and after (red spheres) O_2 exposure. The green line shows the time resolution and the blue line the fit described in the text.

states presumably happens on a much faster time scale but cannot be distinguished in this measurement as the electron distribution has already considerably broadened temporally and energetically before reaching the energy level of C2.

Therefore, we performed experiments with a pump photon energy of $h\nu_{pump} = 2.33$ eV aiming on a direct population of the surface state C2 without prior electron relaxation. For this photon energy, an optical transition to C2 from occupied surface states in the vicinity of the VBM was predicted in DFT calculations by Schmidt *et al.*, in agreement with reflection anisotropy spectroscopy (RAS) measurements of the In-rich InP(100) surface [24]. A contour plot of the corresponding tr-2PPE measurement is shown in Fig. 4(a). The energy range of C2 that was measured before, in the experiments with $h\nu_{pump} = 4.55$ eV [cf. inset Fig. 1(a)], is indicated with a striped bar and clearly overlaps with the photoexcited electron distribution, as expected for an initial resonant population of C2. However, the center of the peak is below C2. We relate this to bulk electrons, photoexcited via interband transitions. Since the heavy-hole band at the Brillouin zone (BZ) center is rather flat compared to the conduction band [35], the electrons take most of the excess energy. Thus, electronic bulk states near C2 are populated, which could also lead to population of C2 through scattering processes.

To clarify this, we once again distinguished between bulk and surface state related signals by comparing measurements before and after oxygen exposure of the sample. Corresponding spectra for different pump probe delays before (black) and after (red) O_2 exposure are presented in Fig. 4(b). After appropriate normalization, they look identical for $\Delta t > 150$ fs and $E_{kin} > 1$ eV. As the signal in this range is unaffected by O_2 exposure, we conclude that it stems completely from bulk electrons. The differences for $E_{kin} < 1$ eV are difficult to disentangle as O_2 exposure also leads to a significant change in the generation rate of secondary electrons and 1PPE.

For $\Delta t < 150$ fs, however, there are remarkable differences between both measurements. The maximum of the electron distribution that forms immediately after excitation is centered 0.1 eV (clean surface), respectively, 0.2 eV (O_2-exposed surface) below the level of C2. We attribute the higher initial peak energy for the clean surface to a resonant population of C2. In Fig. 4(c), we compare transients before and after O_2 exposure for the electrons in the vicinity of C2 with 1.65 eV $< E_{kin} <$ 1.75 eV, where the differences are most pronounced. While the rise time of the signal in both cases reflects the time resolution of the setup, we see clearly different decay behaviors before and after oxygen exposure. The transient of the O_2-exposed sample decays with a time constant of $\tau_{slow} \approx 600$ fs. The clean surface on the other hand shows a rapid decay during the first 150 fs and only for longer time delays, the curve of the clean surface follows the one measured for the O_2 exposure. We fit these data with a simple biexponential model to take into account the slow bulk signal. We used the length of the pump pulse ($\Delta_{fwhm} \approx 33$ fs) as rise time and convoluted the modeled data with a Gaussian curve corresponding to the probe pulse ($\Delta_{fwhm} \approx 27$ fs). The result is plotted in Fig. 4(c) as a blue line, giving a time constant of $\tau_{fast} = 20$ fs for the rapid decay. As this decay only occurs at the clean surface, we attribute the 20-fs time constant to the depopulation of the surface state C2. The signal increases again slightly in the range 200 fs $< \Delta t <$ 300 fs, a feature that was found to be more prominent in measurements with lower pump photon energies and that has been related in previous measurements to electrons returning from the X valley to the Γ valley by intervalley scattering [20].

IV. DISCUSSION

For the tr-2PPE measurements with about 2 eV excess energy, shown in Fig. 2, we observe a prominent signal enhancement at the C2 energy level after ≈200 fs for the clean surface. This is clearly identified as the population of C2 by electrons that relax from higher energetic bulk states. Since the transients from this energy level look very similar for the clean and the O_2-exposed surface, we conclude that the presence of the surface states does not significantly influence the electron cooling. The photoexcited electron distribution ranges several nanometers into the bulk due to the finite absorption coefficient [36] while the surface state extends only about 0.5 nm into the bulk following DFT calculations [31]. Thus, only a small percentage of the photoexcited electrons actually populate the surface states. Consequently, most of the energy loss processes occur inside the bulk and the energy loss rate is not affected by O_2 exposure of the surface and quenching of the surface state C2.

The drastic increase in amplitude for $\Delta t > 300$ fs, that we see in the tr-2PPE signal when the electron distribution reaches C2, relates to a higher probability of electrons in the surface state to be photoemitted and subsequently detected than for electrons in the bulk [37]. This is not unexpected

since most bulk electrons at this energy level populate the four L valleys due to a density of states which is approximately one order of magnitude higher than for the Γ valley, considering the effective electron masses at the valley minima [35]. As the L valleys lie along the [111] directions in $\mathbf{k}$ space, the corresponding photoemitted electrons have a nonzero transversal momentum and are thus not detected with our setup (cf. Sec. II).

In the experiments with a pump photon energy of $h\nu_{pump} = 2.33$ eV, shown in Fig. 4, C2 is populated directly by optical excitation. The rapid drop of the initial amplitude with a time constant of $\tau_{fast} = 20$ fs in the transient of the C2 energy level [cf. Fig. 4(c)] does not appear in the measurement after O_2 exposure of the sample. This strongly indicates that τ_{fast} corresponds to C2-to-bulk scattering since we found out that electrons in C2 have a higher probability of being photoemitted than electrons in the bulk [cf. Fig. 2(b)]. Bulk-to-C2 scattering would thus lead to a rising signal instead, as found for the monochromatic measurements (cf. Fig. 2) and reported by Töben *et al.* in their experiments that focused on the dynamics of C1 [20,21].

With a time constant of $\tau_{fast} = 20$ fs, C2-to-bulk scattering happens on a similar time scale as bulk-to-C1 scattering, determined in previous experiments, where a time constant of $\tau = 35$ fs was measured [21]. These scattering times are also comparable to bulk electron phonon scattering. Schmuttenmaer *et al.*, e.g., found lifetimes of <50 fs for electrons with ≈ 2 eV excess energy for GaAs [14] and for silicon also lifetimes <50 fs were reported [18]. However, for a direct comparison of bulk and surface related scattering it is necessary to take into account that the depopulation of the surface state is not restricted to the emission of optical phonons but can also happen via acoustic phonons and absorption processes. Acoustic phonons have a smaller energy than optical phonons and thus play a minor role in the cooling of the electron distribution near the BZ center [38]. Nevertheless, they may become important for the depopulation of C2 and can explain the short lifetime of electrons in C2, together with the other mechanisms discussed before.

Our measurements show that scattering from surface to bulk states can be extremely efficient and similarly as fast as electron-phonon scattering between bulk states, in particular for electrons with high excess energy where the bulk density of states is also high. Therefore, the presence of surface states at the InP(100) surface is unlikely to slow down electron cooling. An accelerating effect is also not expected when most electrons are located in the bulk. However, in nanostructured devices, a major share of the atoms forms the surface/interface and hence surface states must be taken into account and considered as equally relevant for electron-phonon scattering events as bulk states.

V. CONCLUSION

In experiments with high excitation energies, the surface state C2 is populated and depopulated by bulk electrons that relax towards the conduction band minimum. We observe that the presence of C2 does not have a considerable influence on the relaxation process of the hot electron distribution and that the population of C2 leads to an enhancement in the tr-2PPE spectrum at a specific kinetic energy.

For resonant optical excitation of C2, however, a very fast decaying signal was identified with the depopulation of this surface state. The time constant for scattering events from C2 to surrounding bulk states was measured and we showed that it is similar to bulk scattering processes. As a consequence, electron-phonon scattering scenarios between bulk and surface states might have a significant accelerating effect on the relaxation dynamics for materials with a high surface-to-bulk ratio such as low-dimensional structures.

ACKNOWLEDGMENT

This work was supported by the German Federal Ministry of Education and Research (Grant BMBF 03SF0404B).

[1] F. Dimroth, M. Grave, P. Beutel, U. Fiedeler, C. Karcher, T. N. D. Tibbits, E. Oliva, G. Siefer, M. Schachtner, A. Wekkeli, A. W. Bett, R. Krause, M. Piccin, N. Blanc, C. Drazek, E. Guiot, B. Ghyselen, T. Salvetat, A. Tauzin, T. Signamarcheix, A. Dobrich, T. Hannappel, and K. Schwarzburg, Prog. Photovoltaics **22**, 277 (2014).

[2] H. J. Lewerenz, C. Heine, K. Skorupska, N. Szabo, T. Hannappel, T. Vo-Dinh, S. A. Campbell, H. W. Klemm, and A. G. Muñoz, Energy Environ. Sci. **3**, 748 (2010).

[3] U. Hohenester, P. Supancic, P. Kocevar, X. Q. Zhou, W. Kutt, and H. Kurz, Phys. Rev. B **47**, 13233 (1993).

[4] R. Clady, M. J. Y. Tayebjee, P. Aliberti, D. Knig, N. J. Ekins-Daukes, G. J. Conibeer, T. W. Schmidt, and M. A. Green, Prog. Photovoltaics **20**, 82 (2012).

[5] L. Rota, P. Lugli, T. Elsaesser, and J. Shah, Phys. Rev. B **47**, 4226 (1993).

[6] P. N. Saeta, J. F. Federici, B. I. Greene, and D. R. Dykaar, Appl. Phys. Lett. **60**, 1477 (1992).

[7] A. Cretí, M. Anni, M. Z. Rossi, G. Lanzani, G. Leo, F. D. Sala, L. Manna, and M. Lomascolo, Phys. Rev. B **72**, 125346 (2005).

[8] P. Sippel, W. Albrecht, D. Mitoraj, R. Eichberger, T. Hannappel, and D. Vanmaekelbergh, Nano Lett. **13**, 1655 (2013).

[9] J. Z. Zhang, Acc. Chem. Res. **30**, 423 (1997).

[10] H. Döscher, O. Supplie, M. M. May, P. Sippel, C. Heine, A. G. Muñoz, R. Eichberger, H.-J. Lewerenz, and T. Hannappel, Chem. Phys. Chem. **13**, 2899 (2012).

[11] L. Gundlach, R. Ernstorfer, E. Riedle, R. Eichberger, and F. Willig, Appl. Phys. B **80**, 727 (2005).

[12] M. Weinelt, M. Kutschera, R. Schmidt, C. Orth, T. Fauster, and M. Rohlfing, Appl. Phys. A **80**, 995 (2005).

[13] J. R. Goldman and J. A. Prybyla, Phys. Rev. Lett. **72**, 1364 (1994).

[14] C. A. Schmuttenmaer, C. Cameron Miller, J. W. Herman, J. Cao, D. A. Mantell, Y. Gao, and R. J. D. Miller, Chem. Phys. **205**, 91 (1996).

[15] S. Jeong, H. Zacharias, and J. Bokor, Phys. Rev. B **54**, R17300 (1996).
[16] T. Ichibayashi and K. Tanimura, Phys. Rev. Lett. **102**, 087403 (2009).
[17] J. Azuma, K. Takahashi, and M. Kamada, Phys. Rev. B **81**, 113203 (2010).
[18] M. Mauerer, I. L. Shumay, W. Berthold, and U. Höfer, Phys. Rev. B **73**, 245305 (2006).
[19] L. Töben, T. Hannappel, R. Eichberger, K. Möller, L. Gundlach, R. Ernstorfer, and F. Willig, J. Cryst. Growth **248**, 206 (2003).
[20] L. Töben, L. Gundlach, T. Hannappel, R. Ernstorfer, R. Eichberger, and F. Willig, Appl. Phys. A **78**, 239 (2004).
[21] L. Töben, L. Gundlach, R. Ernstorfer, R. Eichberger, T. Hannappel, F. Willig, A. Zeiser, J. Förstner, A. Knorr, P. H. Hahn, and W. G. Schmidt, Phys. Rev. Lett. **94**, 067601 (2005).
[22] W. G. Schmidt and F. Bechstedt, Surf. Sci. **409**, 474 (1998).
[23] T. Hannappel, L. Töben, S. Visbeck, H. J. Crawack, C. Pettenkofer, and F. Willig, Surf. Sci. **470**, L1 (2000).
[24] W. G. Schmidt, E. L. Briggs, J. Bernholc, and F. Bechstedt, Phys. Rev. B **59**, 2234 (1999).
[25] N. Esser, W. G. Schmidt, J. Bernholc, A. M. Frisch, P. Vogt, M. Zorn, M. Pristovsek, W. Richter, F. Bechstedt, T. Hannappel, and S. Visbeck, J. Vac. Sci. Technol. B **17**, 1691 (1999).
[26] T. Hannappel, S. Visbeck, K. Knorr, J. Mahrt, M. Zorn, and F. Willig, Appl. Phys. A **69**, 427 (1999).
[27] M. M. May, H.-J. Lewerenz, and T. Hannappel, J. Phys. Chem. C **118**, 19032 (2014).
[28] S. Jeon, H. Kim, W. A. Goddard, and H. A. Atwater, J. Phys. Chem. C **116**, 17604 (2012).
[29] B. C. Wood, T. Ogitsu, and E. Schwegler, J. Chem. Phys. **136**, 064705 (2012).
[30] P. Sippel, O. Supplie, M. M. May, R. Eichberger, and T. Hannappel, Phys. Rev. B **89**, 165312 (2014).
[31] W. G. Schmidt, N. Esser, A. M. Frisch, P. Vogt, J. Bernholc, F. Bechstedt, M. Zorn, T. Hannappel, S. Visbeck, F. Willig, and W. Richter, Phys. Rev. B **61**, R16335 (2000).
[32] T. Hannappel, S. Visbeck, L. Töben, and F. Willig, Rev. Sci. Instrum. **75**, 1297 (2004).
[33] T. Hertel, E. Knoesel, M. Wolf, and G. Ertl, Phys. Rev. Lett. **76**, 535 (1996).
[34] G. Chen, S. B. Visbeck, D. C. Law, and R. F. Hicks, J. Appl. Phys. **91**, 9362 (2002).
[35] I. Vurgaftman, J. R. Meyer, and L. R. Ram-Mohan, J. Appl. Phys. **89**, 5815 (2001).
[36] S. Adachi, J. Appl. Phys. **66**, 6030 (1989).
[37] R. Haight, Surf. Sci. Rep. **21**, 275 (1995).
[38] C. Jacoboni, *Theory of Electron Transport in Semiconductors: A Pathway from Elementary Physics to Nonequilibrium Green Functions* (Springer, Berlin, 2010).